*Macromolecular Chemistry and Physics*

Macromolecular Chemistry and Physics
www.mcp-journal.de

REVIEW OPEN ACCESS

# Ferroelectric Properties of Polyvinylidene Fluoride (PVDF): Advances and Prospects for Emerging Applications

Achidi Frick[1] | David Schreuder[1,2,3] | Alejandra Castro-Chong[3,4] | Elizabeth von Hauff[1,3,4]

[1]Department of Physics and Astronomy, Vrije Universiteit Amsterdam, Amsterdam, The Netherlands | [2]Boysen-TU Dresden-Research Training Group, Dresden, Germany | [3]Institute of Solid State Electronics, Faculty of Electrical and Computer Engineering, Dresden Technical University, Dresden, Germany | [4]Fraunhofer Institute for Electron and Plasma Technology FEP, Dresden, Germany

**Correspondence:** Alejandra Castro-Chong (alejandra.castro@tu-dresden.de)

**Received:** 21 July 2025 | **Revised:** 28 November 2025 | **Accepted:** 20 December 2025

**Keywords:** FERAM | memory applications | neuromorphic computation | organic Ferroelectrics | PVDF-TrFE

## ABSTRACT

The growing demand for high-performance consumer electronics and telecommunication devices has driven the development of advanced, efficient, and high-speed data storage solutions. While silicon-based technologies have long dominated the memory market, their physical and performance limitations have spurred interest in alternative materials. Ferroelectric materials, characterized by their ability to exhibit spontaneous and reversible polarization, have emerged as promising candidates for next-generation memory technologies. Among these, polyvinylidene fluoride (PVDF), an organic ferroelectric polymer, has gained attention due to its mechanical flexibility, lightweight nature, non-toxicity, scalability, and ease of fabrication. This review critically evaluates the ferroelectric properties of PVDF and its potential for memory and emerging applications. PVDF's molecular structure, fabrication techniques, and performance in conventional memory technologies, such as FeRAM and FeFETs, are assessed, alongside its limitations compared to inorganic ferroelectrics like lead zirconium titanate (PZT) and hafnium zirconium oxide (HZO). Beyond conventional memory, PVDF's applications in neuromorphic computing and sensing technologies are discussed, where its ferroelectric, piezoelectric, and pyroelectric properties enable artificial synaptic plasticity, real-time detection, and transient data storage. Additionally, PVDF-based composites are examined, highlighting their ability to overcome intrinsic limitations of pure PVDF through the integration of organic and inorganic fillers. While PVDF may not yet match the performance of inorganic ferroelectrics in traditional metrics such as polarization strength and cycle endurance, its versatility, flexibility, and scalability make it a compelling candidate for applications in flexible electronics, biomedical devices, and the Internet of Things (IoT). This review provides a comprehensive assessment of PVDF's role in advancing next-generation memory technologies and multifunctional electronic applications.

## 1 | Introduction

Integrated circuits (ICs) have evolved significantly over the last century, becoming increasingly complex and powerful while steadily decreasing in size. Once confined to research laboratories, ICs are now ubiquitous in modern life, powering consumer electronics, telecommunication devices, and advanced computing systems. Historically, innovation in ICs was driven by the miniaturization of silicon-based devices. However, as silicon technologies approach their physical and performance limits, material science research has shifted toward the development and integration of functional materials to address challenges related to speed, density, size, and cost.

Among these functional materials, ferroelectric materials have emerged as promising candidates for next-generation memory technologies. These materials are characterized by their ability to exhibit spontaneous electric polarization that can be reversed by applying an external electric field that exceeds a material-dependent coercive field [1, 2]. This unique property makes ferroelectric materials attractive for memory devices, which are specialized ICs designed for binary data storage and retrieval.

Ferroelectric materials can be broadly classified into perovskites, other oxides, nitrides, and organic materials, each offering unique properties and challenges for various applications. Perovskite-based systems such as lead zirconium titanate (PZT) and barium titanate ($BaTiO_3$) have long dominated the field due to their exceptional performance [3]. However, their reliance on toxic heavy elements like lead (Pb) and barium (Ba), along with brittleness and high-temperature processing requirements, limits their applicability in flexible, biocompatible, and environmentally friendly systems. Other oxides, such as potassium niobate ($KNbO_3$), which avoids heavy elements, have gained attention, while hafnium zirconium oxide (HZO) has emerged as a CMOS-compatible option. Despite its promise, HZO faces challenges with processing, reproducibility, and material fatigue [4]. More recently, nitrides such as aluminium scandium nitride (Al(Sc)N) have shown potential for integration into microelectronics but require high processing temperatures and specific substrates.

Organic ferroelectric materials offer unique advantages, including lightweight designs, flexibility, non-toxicity, and smooth interfacing with biological systems. They are classified into three categories based on molecular structures: small-molecule organic ferroelectrics, polymer-based ferroelectrics, and supramolecular ferroelectrics [5]. Among polymers, PVDF stands out due to its well-studied ferroelectric phase and ease of processing through chemical derivatives. Here, we focus on PVDF due to its potential for integrating polymeric materials into biocompatible, flexible applications in emerging man–machine technologies, as well as its ability to form structures beyond planar thin films [6, 7]. Furthermore, its tunable ferroelectric properties, achieved through fabrication techniques such as mechanical stretching, electrical poling, and copolymerization, make it highly suitable for advanced memory applications [8–11].

This review critically examines the ferroelectric properties of PVDF and its role in memory and emerging applications, highlighting its potential as a versatile material for next-generation technologies. Section 2 introduces the fundamental principles of ferroelectricity, focusing on dielectric and ferroelectric properties, polarization response and hysteresis, and memory retention and polarization stability. Section 3 examines memory device architectures and operational principles, covering both volatile and non-volatile memory types and memory cell designs. Section 4 categorizes ferroelectric materials into perovskites, oxides, nitrides, and organic ferroelectrics, with a detailed focus on PVDF's molecular structure, polymorphic phases, and fabrication techniques. Section 5 provides a comparative analysis of PVDF-based composites and non-PVDF ferroelectric materials, such as transition metal dichalcogenides and 2D perovskites, highlighting their respective advantages, challenges, and potential for advanced memory applications. Finally, Section 6 explores PVDF's applications beyond conventional memory, including flexible and ferroelectric storage, neuromorphic computing, and sensing technologies. Together, these sections present a comprehensive assessment of PVDF's role in advancing memory and multifunctional electronic technologies.

## 2 | Memory Devices: Architectures and Operational Principles

### 2.1 | Volatile and Non-Volatile Memory Types

Memory devices store information that can be electronically accessed on demand. The smallest component of a memory device is the memory cell, which can switch between two stable, distinct states with a single operation. This bistable nature enables the storage of information in binary form, represented as either 0 or 1. A single binary digit is called a bit, and eight bits make up a Byte. Data communication occurs through an external processing unit, which supplies power to read and write bits.

Memory devices are broadly categorized into volatile and non-volatile types. Volatile memory, such as Static Random Access Memory (SRAM) and Dynamic Random Access Memory (DRAM), offers rapid data access but requires a constant power supply to retain information. Non-volatile memory, such as Flash and Ferroelectric Random Access Memory (FeRAM), can retain data without power, making it ideal for applications requiring extended data retention, large storage capacity, and low power consumption [12–14]. Each type of memory serves distinct purposes in computer systems. For example, read-only memory (ROM) is used to reliably retain small amounts of data required for basic functions before the operating system boots up. Meanwhile, Flash memory provides long-term storage, and SRAM and DRAM enable rapid data access and processing. The circuit diagrams of common memory devices are shown in Figure 1.

Volatile RAM is characterized by rapid, short-term storage capabilities, allowing data to be written or read in any order. The simplest RAM cell architecture consists of a single transistor and a capacitor, although more complex architectures exist [15]. However, adding extra components within a cell reduces memory density by increasing cell size, which also raises costs. DRAM, with its simpler architecture, requires periodic refreshing of stored data due to charge leakage in the capacitor. In contrast, SRAM eliminates the need for refreshing but relies on a more complex architecture, enabling faster read/write operations at the expense of higher power consumption and lower memory density. A qualitative overview comparing the characteristic memory parameters for SRAM, DRAM, Flash, and FeRAM is shown in Figure 1e. Emerging variations of RAM, such as FeRAM, Magneto-Resistive RAM (MRAM), and Phase-Change RAM (P(C)RAM), offer promising alternatives but are not yet commercially available [16, 17].

Non-volatile memory is primarily used for long-term data storage and is slower than volatile memory. Flash memory, one of the most widely used non-volatile formats, consists of an array of memory cells resembling floating-gate MOSFETs (Metal-Oxide Semiconductor Field Effect Transistors). Flash memory cells

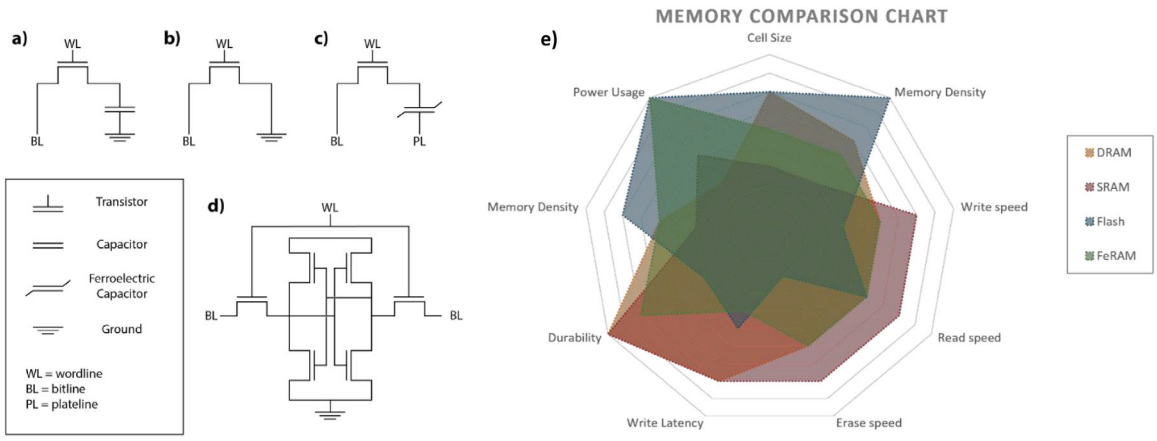


**FIGURE 1** | Circuit diagrams for a) DRAM, b) Flash, c) FeRAM, and d) SRAM single memory cells. Electrodes and extra circuit elements shown in d) are left out in this schematic representation. e) Qualitative overview of the characteristic memory parameters for SRAM, DRAM, Flash, and FeRAM.

include a control gate stacked above the floating gate, which acts as a voltage-dependent switch to inject charge into the floating gate, where information is stored via trapped charge [18]. Flash memory can retain multiple bits of data in a single cell, known as multi-level cells (MLC), which can be further extended to triple-level cells, quad-level cells, and penta-level cells [2, 19]. However, Flash memory cannot write and erase data in any order; an entire data block must be erased before new data can be recorded. Additionally, Flash memory has a finite number of erase cycles ($<10^6$ P/E cycles), although advances in self-healing materials may improve this parameter [20]. Despite its lower cost per bit and resistance to material defects, Flash memory is one to two orders of magnitude slower than volatile memory, making it less suitable for repetitive tasks requiring high-speed operation.

## 2.2 | Memory Cell Architectures

Memory cells are composed of transistors (T) and capacitors (C), which serve as the fundamental units for writing, reading, and storing data. Common architectures include DRAM and FeRAM, which consist of a single capacitor and transistor, although more complex configurations such as 2T-2C or 2T-1C also exist [17]. SRAM cells are more sophisticated, often incorporating 4–10 transistors, and may include additional resistors (2R) to enhance functionality [18]. Consequently, SRAM cells are approximately six times larger than DRAM cells, limiting their memory density.

Memory cells are typically integrated into multi-cell structures, such as crossbar arrays. These arrays consist of memory cells packed into a 2D grid sandwiched between perpendicular wordlines and bitlines. Stacked arrays enable high-capacity memory devices, although memory density is constrained by the physical distance between individual cells. Wordlines provide access to specific cells in the array, while bitlines deliver the voltage required for reading and writing data. Despite architectural similarities between DRAM and FeRAM, FeRAM requires an additional plateline or driveline to regulate the electric field across the ferroelectric capacitor during memory cycles. The plateline acts as a global electrode, assisting in both reading and writing operations [21]

In complex memory architectures, the minimum cell size ($F$) is often relatively large, which limits memory density. High-density memory is essential for applications requiring substantial storage capacity and compact form factors, such as data centers and smartphones. For applications with lower data capacity, reducing cell size may seem less critical from a user perspective. However, from a design standpoint, shrinking cell size remains relevant as it enables new form factors, reduces cost per bit, and unlocks additional use cases.

Among ferroelectric memory devices, FeRAM and ferroelectric field-effect transistors (FeFET) are the most intensively researched [22]. FeRAM relies on the polarization state of ferroelectric materials for data storage, rather than charge storage in a capacitor. FeRAM combines many desirable properties, including compact size, relatively high speed, and low cell complexity. While its memory density is lower than Flash memory, it is comparable to DRAM. FeRAM consumes significantly less power than DRAM, as ferroelectric dielectrics retain data without requiring a constant voltage [23]. In contrast, DRAM retains its charged state only when an external voltage is maintained. FeRAM has already found applications in radio-frequency (RF) tags and microprocessors [24]. Notably, FeRAM was used in Toshiba's Emotion Engine CPU for the Sony PlayStation 2 in 2000. However, subsequent gaming consoles reverted to DRAM-based CPUs, and FeRAM has since seen limited use in mainstream consumer electronics [25, 26].

FeRAM's read cycle is destructive, requiring an additional rewriting step that increases switching events and potentially limits its lifetime. FeFETs, on the other hand, execute read-out via channel conductance modulation, eliminating the need for data rewriting and reducing switching events. This mechanism relaxes the remanent polarization ($P_r$) requirements but is still constrained by polarization fatigue, imprint, and switching kinetics, which impact endurance and speed [27, 28]. Due to FeRAM's slow data transmission, conventional high-speed memory solutions like SRAM and Flash remain faster than FeRAM. Flash memory also offers higher memory density at a lower cost. Despite these advantages, FeRAM suffers from material fatigue in the ferroelectric layer, which typically manifests after far more P/E cycles than Flash endurance ($10^9$–$10^{12}$ cycles for FeRAM vs.

**TABLE 1** | Overview of the characteristic memory parameters for commonly used memory architectures (SRAM, DRAM, Flash) and emerging memory devices.[90, 97–99]

| Qualitative comparison of memory devices (DRAM, SRAM, Flash, and FeRAM) | | | | |
|---|---|---|---|---|
| | **DRAM** | **SRAM** | **Flash** | **FeRAM** |
| Architecture | 1T-1C / 2T-2C / 2T-1C / 3T-1C (Intel 1103) | 6 - 10T-2C / 4T-2R-2C | 1T | 2T-2C / 2T-1C |
| Cell size ($F^2$) [23] | 8–12 | 50–80 | 4–11 | 4–16 |
| Memory density | Medium high | Low | Very High | Medium |
| Write speed [23] | Medium | Fast | Slow | Medium |
| Read speed [23] | Medium | Fast | Medium | Medium |
| Erase speed [23] | Medium | Fast | Very Slow (Entire block) | Medium |
| Read cycle | 1T: Destructive 3T: Non-destructive | Non-destructive | Non-destructive | Destructive |
| Write Latency [44, 57, 100] | Low | Low | Medium (NOR)/High (NAND) | High |
| Overwrite [23] | Direct | Direct | Indirect | Direct |
| Cycle endurance | Unlimited | Unlimited | $10^6$–$10^8$ | $10^{15}$ cycles |
| Memory Density | Medium | Low | High | Medium |
| Volatility | volatile | Volatile | nonvolatile | Nonvolatile |
| Power usage | High | Low-high (depending on accessing frequency) | Very low | Very Low |
| Scalability limits [23] | Capacitor | 6 Transistors | High voltage/Tunnel oxide | Capacitor |

$10^4$–$10^6$ cycles for Flash) [4]. Direct cycle-count comparisons should be interpreted cautiously, as the failure mechanisms differ fundamentally. Table 1 summarizes the parameters of different memory architectures.

## 3 | Ferroelectricity: Principles and Mechanisms

### 3.1 | Dielectric and Ferroelectric Properties

The electrical polarization of a material under an externally applied electric field is a fundamental phenomenon that underpins the operation of solid-state devices. In conductors, the applied electric field induces the flow of charge, dissipating electrical energy. In dielectrics, however, the electric field causes a change in the material's polarization, which depends on its polarizability ($\alpha$). Polarizability is defined as:

$$\alpha = p/E \tag{1}$$

where $p$ is the total dipole moment in the solid, and $E$ is the applied electric field. Microscopically, polarizability is linked to the displacement of ionic (atomic) or dipolar (molecular) species. When a static electric field is applied, dielectric materials exhibit charge displacement ($D$):

$$D = \varepsilon E \tag{2}$$

which gives rise to polarization ($P$):

$$P = \varepsilon E \chi \tag{3}$$

where $\varepsilon$ is the static permittivity and $\chi$ is the susceptibility of the material. The total polarization is determined by the alignment of individual dipole moments within the bulk. For linear dielectrics, $D$ and $P$ are directly proportional to the strength of the applied electric field. When the field is removed, the polarization vectors relax to an anisotropic state, resulting in $P = 0$.

In contrast, ferroelectric materials exhibit a non-centrosymmetric crystalline phase, which leads to anisotropic polarization vectors and a non-zero net polarization even in the absence of an external electric field. Two critical parameters define ferroelectric behavior: the coercive field ($E_c$), which is the electric field strength required to reverse the direction of spontaneous polarization, and the Curie temperature ($T_c$), which marks the transition from the ferroelectric phase to the paraelectric phase. Above $T_c$, dipole moments are distributed isotropically, and as the temperature approaches $T_c$, $E_c$ decreases, resulting in a narrower hysteresis loop. Relaxor ferroelectrics, which contain small, unstable ferroelectric domains, exhibit polarization relaxation over time, decreasing the total polarization. These materials are advantageous for applications requiring low-voltage operation or high-energy storage density, although they often require material engineering to ensure polarization stability for memory applications [29].

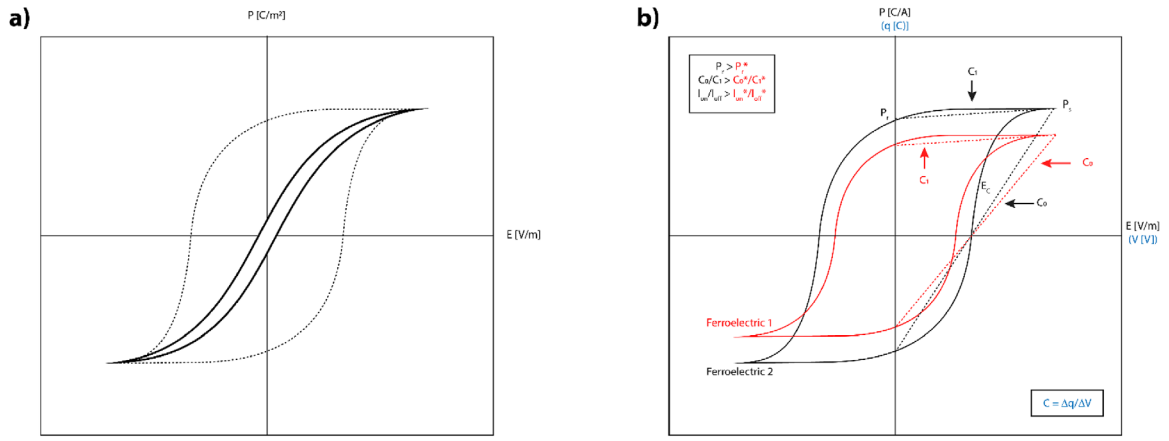


**FIGURE 2** | a) Polarization curve of a ferroelectric relaxor (solid line) and a conventional ferroelectric (dashed line) [17]. b) Two ferroelectric hysteresis curves observed in experiments. The axis can be represented as either ferroelectric parameters (black) or the closely related parameters (blue, related via $V = \mathrm{Ed}$, $q = \mathrm{PA}$) relevant at reading operations in FeRAM. The fraction of the slopes of the state-dependent capacitance ($C = q/V$) scales with the retention time of the current ($I_{on}/I_{off}$). Therefore, the black curve contains a higher retention time of $I_{on}/I_{off}$ [15, 49].

The difference between a relaxor and a conventional ferroelectric is depicted in Figure 2a. The advantage of relaxor ferroelectrics for device applications (e.g., ferroelectric tunnel junction [30]) is that polarization can be switched at lower voltages compared to conventional ferroelectrics. While this enables applications requiring low-voltage operation or high-energy storage density, it often necessitates specific material engineering to ensure sufficient polarization stability for memory applications.

### 3.2 | Polarization Response and Hysteresis

The polarization response of ferroelectric materials is commonly represented by a quasi-static polarization-electric field (*PE*) hysteresis loop. This loop is measured by applying a slow (<1 Hz) alternating electric field to induce polarization switching. The hysteresis loop provides key parameters, including the coercive field ($E_c$), remanent polarization ($P_r$), and saturated polarization ($P_s$). $E_c$ is defined as the field strength at $P = 0$, $P_r$ is the polarization at $E = 0$, and $P_s$ is the maximum polarization achieved at the highest applied field. The magnitude of $P_s$ depends on the external field strength used during measurement. For device applications, the applied voltage ($V$) is plotted on the $y$-axis instead of $E$, where $E = V/d$ and $d$ is the thickness of the ferroelectric layer [31–33]. A common representation of the polarization response is shown in Figure 2b, which is a quasi-static *PE* hysteresis loop measured while applying a slow (< 1 Hz) alternating electric field to switch the polarization.

The switching dynamics of polarization can be evaluated by varying the frequency of the alternating voltage. The highest frequency at which ferroelectric switching occurs corresponds to the polarization switching frequency. The time-dependent polarization change can be described by the Merz equation:

$$\tau = Ae^{\left(\frac{E_a}{E}\right)} \tag{4}$$

where $\tau$ is the ferroelectric switching time constant, $A$ is the lower limit of switching time ($E \to \infty$), $E_a$ is the activation field for switching, and $E$ is the applied field. The evolution of polarization over time $P(t)$ can be expressed as:

$$P(t) = 2P_r\left(1 - e^{-\left(\frac{t}{\tau}\right)^n}\right) \tag{5}$$

where $\tau$ is the switching time constant, and $n$ is the Avrami index, which is sample-dependent. Experimental hysteresis loops of ferroelectrics align well with this equation, providing insights into switching kinetics and polarization stability [34].

### 3.3 | Memory Retention and Polarization Stability

Memory retention is a key parameter that determines the operational lifetime of memory cells. It refers to the duration over which binary states remain distinguishable and is directly correlated with $P_r$. To probe the polarization state, a reading voltage pulse ($V_r$) is applied. In FeRAM, $V_r$ is typically equal to the switching pulse. If the initial polarization state is parallel to the electric field induced by $V_r$ (Off state), the polarization remains unchanged, and the reading process is non-destructive. Conversely, if the initial polarization is antiparallel to the field (On state), the polarization switches, making the reading process destructive. For reliable operation, the current retention ratio ($I_{on}/I_{off}$) must be sufficiently large to allow the sense amplifier to differentiate between binary states [35, 36]. The retention time of the current ($I_{on}/I_{off}$) is compared for two hysteresis curves in Figure 2b.

Memory retention can degrade due to phenomena such as fatigue, aging, imprinting, or elevated temperatures. Fatigue refers to the gradual decrease in $P_r$ as a function of polarization cycles, which is irreversible in FeRAM due to its destructive readout mechanism. Aging is the loss of polarizability over time, accompanied by an increase in hysteresis, which reduces the difference between bistable states. Imprinting occurs when one bistable state loses polarizability after prolonged retention in the opposite state. Elevated temperatures can further degrade performance by lowering $E_c$ and transforming the ferroelectric phase into the paraelectric phase [21].

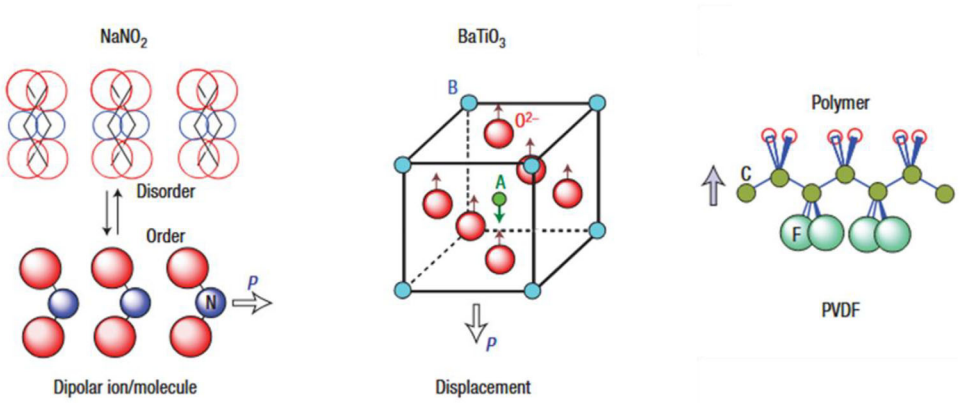


**FIGURE 3** | Schematic drawings of $NaNO_2$, $BaTiO_2$, and PVDF illustrating their ferroelectricity mechanism at the microscopic level. Adapted with permission. [9] 2008, Nature Publishing Group.

To evaluate the lifetime of FeRAM devices, consecutive polarization switching cycles (P/E cycles) are applied to monitor fatigue and aging. The cycle-by-cycle response is typically summarized as a plot of the current ratio ($I_{on}/I_{off}$) versus time at a fixed operation frequency. Reported endurance windows for FeRAM vary widely, ranging from $10^6$ to $10^{15}$ P/E cycles, depending on the material. PZT-based devices often achieve higher endurance, while HZO-based devices excel in scalability and low-voltage operation [1, 37, 38]. Accelerated tests, conducted at operation frequencies of up to ~1 MHz, provide insights into long-term device reliability.

## 4 | Classes of Ferroelectric Materials

Ferroelectric materials, characterized by their spontaneous and reversible electric polarization, have garnered significant attention for their applications in memory devices, sensors, actuators, and energy harvesting systems. These materials can be broadly classified into four major categories: perovskites, oxides, nitrides, and organic ferroelectrics. Each class exhibits unique structural and functional properties, offering distinct advantages and challenges for various applications. At the microscopic level, there are different mechanisms through which these materials achieve ferroelectricity, i.e., spontaneous polarization due to (i) the permanent dipoles of molecules or ions (e.g., $NaNO_2$, PVDF), (ii) relative displacement of ions (e.g., perovskites such as $BaTiO_3$), or (iii) dynamic protons in hydrogen bonds (e.g., $KH_2PO_4$ (KDP)). In Figure 3, schematic drawings of the ferroelectric materials assessed in this review are presented [9].

A special class of ferroelectric materials is the molecular ferroelectrics, which, owing to their advantages of lightweight, biocompatibility, structural tunability, and mechanical flexibility, have emerged in the past decade as promising complementary materials to commercial inorganic ferroelectrics. Here, we won't address this class in detail [39].

### 4.1 | Perovskite Ferroelectrics

Perovskites, with the general formula $ABO_3$, are among the most extensively studied ferroelectric materials due to their highly tunable crystal structure, which allows for a wide range of compositions and properties. Prominent examples include PZT, barium titanate ($BaTiO_3$), and strontium titanate ($SrTiO_3$). These materials are characterized by high dielectric constants, strong piezoelectric and pyroelectric properties, and robust ferroelectric behavior, making them essential for applications such as non-volatile memories, capacitors, actuators, and transducers. However, the presence of lead in PZT raises environmental concerns, driving efforts to develop lead-free alternatives. Additionally, perovskites often require high-temperature processing, with PZT, for instance, necessitating annealing temperatures of around 600°C. Despite these challenges, perovskites remain a cornerstone of ferroelectric research and applications due to their exceptional performance [3, 40].

### 4.2 | Oxide Ferroelectrics

Oxide ferroelectrics include a diverse range of materials, such as tungsten bronzes, layered perovskites, and binary oxides like hafnium oxide ($HfO_2$). The most notable example is HZO, which is highly valued for its thermal stability, compatibility with semiconductor processing, and potential for miniaturization, making it widely used in microelectronics, energy storage devices, and sensors. However, it often requires high-temperature processing, necessitating annealing temperatures of around 400°C, which limits its compatibility with flexible substrates and low-cost fabrication methods. Additionally, challenges such as complex manufacturing processes and potential fatigue or degradation over time must be overcome to fully unlock its potential in advanced applications [4].

### 4.3 | Nitride Ferroelectrics

Nitride ferroelectrics, such as aluminium scandium nitride (Al(Sc)N), represent an emerging class of materials with promising properties. These materials typically exhibit a wurtzite crystal structure and combine ferroelectricity with high mechanical robustness and chemical stability. Al(Sc)N, in particular, has shown potential for integration into microelectronics due to its compatibility with existing fabrication processes. Applications include piezoelectric sensors, actuators, and RF devices. However, the high processing temperatures and the requirement for

specific substrates pose challenges for large-scale production and integration [41].

### 4.4 | Organic Ferroelectrics

Organic ferroelectrics, including small-molecule crystals, polymers, and supramolecular structures, are increasingly studied for their lightweight, flexible, and biocompatible properties [43, 44]. Their ferroelectric behavior arises from mechanisms such as molecular dipole alignment, hydrogen bonding, or self-assembly [5]. Among these, polyvinylidene fluoride (PVDF) and its copolymers are particularly notable due to their ease of processing and tunable ferroelectric properties, which can be optimized through techniques like mechanical stretching, electrical poling, and copolymerization. However, organic ferroelectrics typically have lower thermal stability and dielectric constants compared to inorganic materials, which limits their application in high-performance systems. To address this, researchers have explored 3D electrode architectures to enhance storage density, where organic ferroelectrics like PVDF offer distinct advantages due to their versatile processing capabilities and ability to form high-density 3D structures [42–47].

#### 4.4.1 | PVDF

In contrast to inorganic and organic crystals, polymers offer unique advantages, including mechanical flexibility, lightweight properties, low-temperature processability, and chemical stability. These features make PVDF particularly attractive for applications such as wearable electronics, biomedical devices, and IoT technologies, where conventional materials like PZT and HZO face significant limitations [6, 9, 10].

PVDF is polymorphic, and the electroactive properties, including ferroelectricity, arise from the $\beta$-phase. This phase is characterized by a non-centrosymmetric crystal structure that enables spontaneous polarization and switching behavior under an electric field [26]. Other phases of PVDF, such as $\alpha$, $\gamma$, $\delta$, and $\varepsilon$, are more difficult to fabricate and lack significant ferroelectric performance, making them unsuitable for memory applications [48–51]. PVDF's distinct phases are shown in Figure 4a,b.

PVDF chains can adopt different conformations depending on the crystalline phase, including trans (T) and gauche (G) configurations [52]. For example:

- **$\alpha$-phase**: TGTG' conformation, thermodynamically stable but non-ferroelectric due to its centrosymmetric structure.
- **$\beta$-phase**: TTTT conformation, non-centrosymmetric with strong ferroelectric, piezoelectric, and pyroelectric properties.
- **$\gamma$-phase**: TTTGTTTG' conformation, ferroelectric but less studied and less pronounced in properties compared to the $\beta$-phase.

The unit cell of the $\beta$-phase, shown in Figure 4c, belongs to the orthorhombic crystal system (space group Cc2m) and exhibits lattice dimensions $\boldsymbol{a = 8.58}$ Å, $\boldsymbol{b = 4.90}$ Å, and $\boldsymbol{c = 2.26}$Å, where $c$ is parallel to the longitudinal chain direction. The zigzag structure of PVDF chains results in deflection angles ($\sigma$), which increase the intrachain fluorine distance from 2.50 to 2.60 Å, further influencing the packing density and polarization properties of the material. This unique molecular arrangement highlights the structural basis for PVDF's ferroelectric behavior and its potential for flexible and scalable electronic applications [52]. However, achieving a high fraction of $\beta$-phase crystallinity is challenging, as PVDF naturally crystallizes in its thermodynamically stable $\alpha$-phase, which lacks ferroelectric properties. Specialized fabrication techniques, such as mechanical stretching, electrical poling, and copolymerization with trifluoroethylene (TrFE), are critical for inducing and stabilizing the $\beta$-phase [53, 54].

**TABLE 2** | Lattice constants for the $\beta$-phase of PVDF and PVDF:TrFE.[73, 75, 101]

| | Lattice constants | | |
|---|---|---|---|
| | **a (Å)** | **b (Å)** | **c (Å)** |
| PVDF | 8.58 | 4.90 | 5.12 |
| PVDF-TrFE (80:20) | 8.90 | 5.05 | 5.10 |
| PVDF-TrFE (70:30) | 9.05 | 5.12 | 5.10 |

*Numbers for *c*-axis in PVDF (80:20) and (70:30) are reported to be c = 2.55 Å, but here we assume a "double" unit cell (cdoubled = 2·c = 5.10 Å).

A fundamental challenge associated with PVDF in memory applications is that very large electric fields are required to induce polarization inversion. In contrast to ionic displacement in inorganic ferroelectrics, polarization inversion involves rotation of the polymer unit cell, and the dynamics involve a much higher energy barrier (for PVDF, $E_c > 100$ MV/m) than for inorganic piezoelectrics. Mechanical stretching aligns PVDF chains along the stretching direction, promoting $\beta$-phase formation. Electrical poling applies a high electric field to orient dipoles and enhance ferroelectric behavior. Copolymerization with TrFE modifies PVDF's molecular structure, reducing steric hindrance and stabilizing the $\beta$-phase [28, 55]. Altering the chemical structure of the PVDF chain is a common strategy to decrease the coercive field, e.g., with the addition of functionalized monomers within the PVDF backbone. Commonly used functional monomer groups are TrFE or Chlorofluoroethylene (CFE), in which a fluoride and chlorine replace one hydrogen atom, respectively. As a consequence, the $\beta$-phase unit cell increases slightly with respect to that of PVDF. In Table 2, the lattice constants for the $\beta$-phase of PVDF and PVDF:TrFE at different concentrations are shown.

Additionally, PVDF-based composites incorporating inorganic fillers (e.g., $Cu_2O$) or hybrid materials have emerged as viable strategies to further enhance ferroelectric performance [56]. These techniques have been foundational in optimizing PVDF's ferroelectric properties, enabling its application in advanced electronic devices. However, new strategies have emerged to enhance $\beta$-phase formation and stability, including the use of PVDF-based composites with inorganic, organic, or hybrid fillers. These advancements, along with

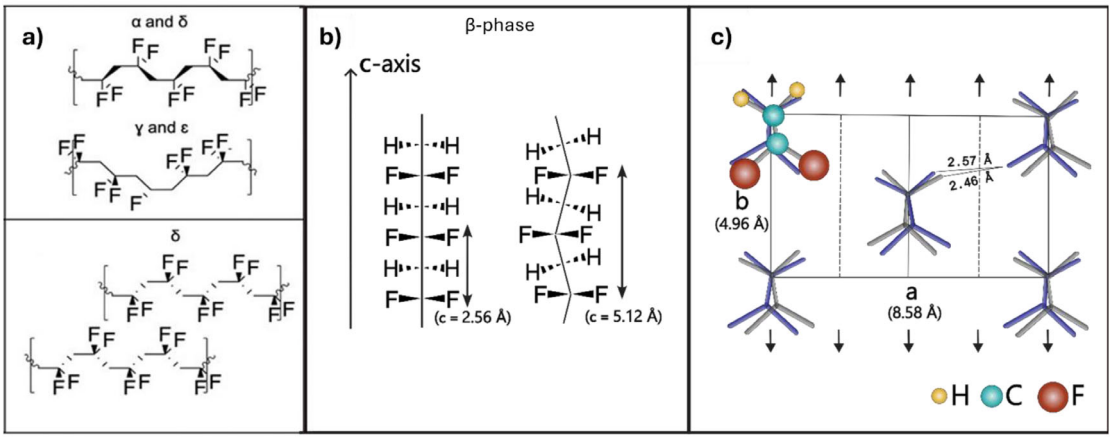


**FIGURE 4** | a) Molecular conformation of the five PVDF phases ($\alpha$, $\gamma$, $\delta$, and $\varepsilon$) in single-chain representation. b) Schematic representation of differences in flat and deflected molecular configurations of the $\beta$-phase, the latter one requiring two monomers instead of one to describe the unit cell. Due to reorientation of atoms in the deflection model, the $c$-axis distance (5.12 Å) is exactly twice the value of the $c$-axis distance of the flat zigzag structure containing a single monomer (2.60 Å). c) Unit cell structure of the non-centrosymmetric $\beta$-phase [52].

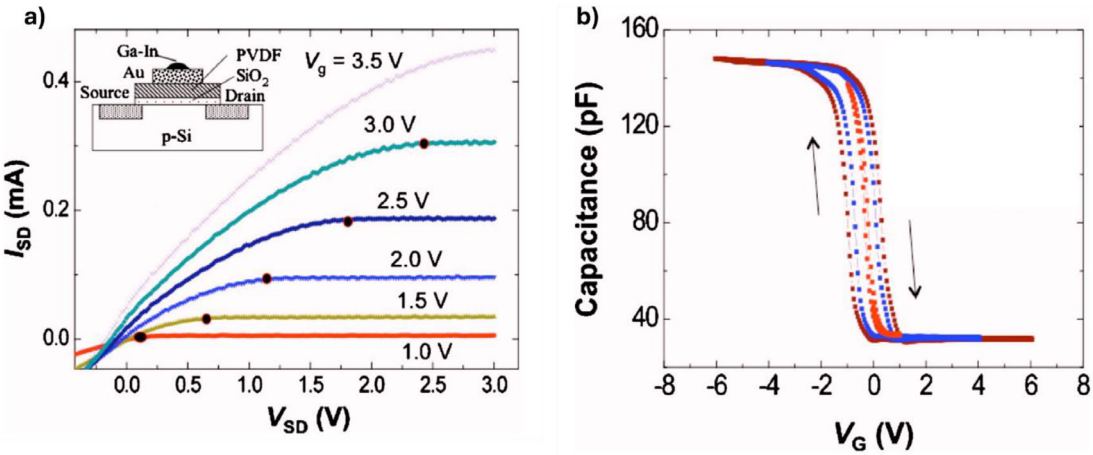


**FIGURE 5** | a) Source-drain current $I_{SD}$ vs $V_{SD}$ curves for an Au/PVDF/$SiO_2$/p-Si FeFET and device diagram ($V_g$ is gate voltage). b) Capacitance-voltage hysteresis loops of a metal-ferroelectric-insulator-semiconductor (MFIS) stack diode. Adapted with permission. [58] 2010, American Institute of Physics, DigitalCommons@University of Nebraska - Lincoln.

their results and associated challenges, are assessed in Section 5.1.

Compared to well-studied ferroelectric oxides like PZT and HZO, PVDF provides several unique advantages. Its lightweight nature, mechanical flexibility, and compatibility with low-temperature processing make it particularly well-suited for applications requiring flexible or wearable electronics. PVDF's chemical stability and non-toxicity provide a distinct edge for biocompatible and environmentally sustainable technologies [6, 7, 11, 24, 57]. A test of the state bistability of a PVDF/$SiO_2$ FeFET is shown in Figure 5a, probed by measuring the source-drain current $I_{SD}$ as the gate voltage $V_g$ increases: flat saturation currents are an indication of low leakage. Figure 5b shows measurements of device capacitance $C$ versus gate voltage $V_g$ in a metal-ferroelectric-insulator-semiconductor MFIS. Accumulation is attained at negative gate bias, resulting in a high device capacitance, while depletion is achieved at positive gate bias, resulting in low capacitance. [58]

Nevertheless, PVDF's ferroelectric performance is less competitive than that of PZT and HZO in key metrics. For example:

- **PZT:** $P_r$ values of 30–75 μC/cm$^2$, $E_c$ as low as 5–10 MV/m, and cycle endurance exceeding $10^{15}$ switching events [6].
- **HZO:** $P_r$ values of 10–30 μC/cm$^2$, $E_c$ values of ~200 MV/m, and scalability to ultrathin layers as small as 5 nm [7].
- **PVDF:** $P_r$ values of 0.1–10 μC/cm$^2$, $E_c$ values of 50–200 MV/m, and cycle endurance comparable to Flash memory (~$10^7$ cycles) [34, 59].

These performance limitations stem from PVDF's polymer backbone, as ferroelectric switching relies on chain rotation for polarization inversion, resulting in higher energy barriers and slow times for switching. In contrast, ferroelectric switching in inorganic crystals relies on ionic displacement.

PVDF's ferroelectric properties stem from its molecular structure combined with optimized fabrication routes. This may pose a limitation in conventional ferroelectric applications, such as FeRAM and FeFETs, but can enable tailoring to application-specific challenges. PVDF's unique properties have potential for adoption in emerging fields such as neuromorphic computing and sensing technologies, which are discussed in Section 6. These applications leverage PVDF's ferroelectric, piezoelectric, and pyroelectric properties to achieve functionalities that extend beyond traditional memory storage. In the next Section, we provide a comparison of the achievements and challenges of PVDF vs alternative ferroelectrics.

## 5 | PVDF Versus Alternative Ferroelectrics: A Comparative Analysis for Memory and Emerging Applications

As the demand for higher performance, scalability, and multifunctionality in emerging memory applications continues to grow, researchers are intensively investigating new material classes with distinct properties that offer advantages and limitations in different application scenarios. We categorize emerging ferroelectrics into two principal groups here: PVDF-based composites and non-PVDF-based ferroelectric materials. In the case of PVDF-based composites, the filler materials, which can be either inorganic or hybrid organic–inorganic, are employed to enhance the properties of the PVDF matrix. For non-PVDF-based ferroelectric materials, the alternatives are typically fabricated as single layers, with 2D materials emerging as the most promising within this category. In this section, we provide a comparative analysis, highlighting their potential to address the limitations of pure PVDF in advanced memory applications.

### 5.1 | PVDF-Based Composites: Enhancing PVDF's Ferroelectric Limitations

While pure PVDF exhibits specific attributes, such as mechanical resilience and suitability for flexible device architectures, its relatively low dielectric constant, limited energy density, and polarization strength restrict its performance in high-capacity and energy-efficient memory systems. To overcome these limitations, PVDF-based composites incorporating organic and inorganic fillers have emerged as a promising solution. By integrating materials such as $BaTiO_3$, ZnO, and 2D perovskites, these composites exhibit enhanced piezoelectric coefficients, increased $\beta$-phase content, and improved dielectric properties, enabling superior functionality for advanced memory applications.

According to the effective medium theory, the incorporation of piezoelectric materials with a high dielectric constant and piezoelectric coefficient significantly influences the molecular alignment and polarization within the polymer matrix. This interaction leads to a substantial enhancement in the piezoelectric performance of the composite material [60]. Already in 1996, Gregorio et al. demonstrated that the addition of $BaTiO_3$ into PVDF composites resulted in a 40 vol.% increase in $\beta$-phase content compared to pure PVDF. This increase in $\beta$-phase content corresponded to an improvement in the relative permittivity of the material, highlighting the effectiveness of $BaTiO_3$ as a functional filler in enhancing polymer matrix properties [61].

Further advancements were reported in 2020 by Park et al., who showed that these changes in molecular polarization led to a 1.5-fold enhancement in overall polarization and a dielectric constant that was 101% higher than $BaTiO_3$-free samples. This significant improvement positioned PVDF-$BaTiO_3$ composites as a highly suitable material for high-capacitive storage applications [62]. Another noteworthy example is zinc oxide (ZnO), which is widely recognized as an effective inorganic piezoelectric material with a high dielectric constant and piezoelectric coefficient. In 2023, Joshi et al. demonstrated that the incorporation of ZnO nanoflowers into the polymer matrix led to a substantial increase in output voltage from 500 to 600 mV. This enhancement in output voltage enabled the material to achieve more robust polarization states, which are critical for reliable data retention in non-volatile memory applications such as FeRAM [63].

Two-dimensional (2D) perovskites have recently gained attention as promising ferroelectric materials due to their unique crystalline structure, which promotes well-aligned molecular dipoles. This arrangement enables exceptional properties, such as intrinsic ferroelectricity, spontaneous polarization, and high piezoelectric responses, making them ideal for advanced ferroelectric PVDF-based composites [64]. In 2024, Chen et al. reported that embedding 2D $(C_4H_9NH_3)_2CsPb_2Br_7$ perovskite nanosheets into PVDF resulted in a 92.8% electroactive $\beta$-phase content and a nearly 1600% increase in output voltage. The composite exhibited a high piezoelectric coefficient ($d_{33}$) of 63.3 pm/V, which is 2.9 times higher than that of pure PVDF (21.7 pm/V), demonstrating its suitability for applications in wireless sensing networks and actuating devices [65]. Furthermore, in 2025, Son et al. developed a self-rectifying resistive memory device. This resistive memory, composed of Ag/PVDF-TrFE:$(BA_2)PbI_4$/indium tin oxide, demonstrated a high resistance switching ratio of $>10^6$ programmable at $\pm$0.4 V, along with an excellent rectification ratio of $>10^6$ at $\pm$0.1 V, long data retention, and stable endurance cycles, showcasing its potential for high-performance non-volatile memory applications [66].

Antiferroelectric materials, particularly single-crystalline systems, have been employed as inorganic fillers to enhance density and improve energy storage performance in PVDF-based composites. In 2023, Chen et al. successfully incorporated $PbZrO_3$ membranes into a PVDF matrix to develop a 2D–2D type composite, achieving an ultrahigh energy density of 43.3 J/cm$^3$ at 750 MV/m, which was 238% higher than that of pure PVDF (18.2 J/cm$^3$ at 500 MV/m) [67]. This higher energy density enables piezoelectric materials to store and release more energy per unit volume, directly influencing polarization switching behavior, which is critical for data storage and retrieval in memory applications.

PVDF-based composites represent an important step forward in addressing the performance limitations of pristine PVDF, offering improved ferroelectric and piezoelectric properties through the integration of organic and inorganic fillers. These enhancements

open up the possibility for application of PVDF in memory applications that require high energy density, improved polarization, and increased dielectric performance. However, the complex fabrication, including maintaining filler dispersion and interfacial stability, poses significant barriers for scalability. Further, the incorporation of heavy elements in the fillers limits application in technologies requiring biocompatibility and non-toxicity. PVDF:TRFE copolymers, while less flexible in terms of property customization, provide simplified, scalable fabrication combined with reliable performance for flexible device architectures that do not require superior ferroelectric performance.

### 5.2 | Emerging Non-PVDF Ferroelectrics: Comparative Advantages and Challenges

While PVDF-based ferroelectrics offer unique advantages such as mechanical flexibility, lightweight design, and low-temperature processability, emerging non-PVDF ferroelectric materials, including transition metal dichalcogenides (TMDs), perovskite oxides, and 2D hybrid organic–inorganic perovskites (HOIPs), have demonstrated superior performance in key metrics. These materials exhibit higher dielectric constants, stronger polarization, and enhanced thermal stability, making them attractive for high-density, energy-efficient memory applications.

TMDs, such as molybdenum disulfide ($MoS_2$), are characterized by diverse crystal structures (e.g., 2H, 3R, and 1T polytypes) and properties like large hysteresis, high ON/OFF ratios, and stable retention, which make them suitable for various memory technologies, including FeRAM and Flash memory [68]. Similarly, perovskite ferroelectrics, such as $PbZr_xTi_{1-x}O_3$ (PZT), are widely used due to their exceptional polarization (up to 75 μC/cm$^2$), reliable operation over $10^{10}$ cycles, and potential for neuromorphic computing applications [69, 70]. However, their reliance on toxic heavy metals and high-temperature processing limits their applicability in flexible and biocompatible devices.

2D HOIPs have emerged as promising candidates for ferroelectric applications due to their high Curie temperatures and large piezoelectric responses. Recent advancements, such as the development of (4,4-difluoropiperidinium)$_2GeBr_4$ with a saturation polarization of 15 μC/cm$^2$ and a Curie temperature of 401 K, highlight their potential for high-performance memory devices [71]. Despite these improvements, challenges such as low spontaneous polarization, environmental sensitivity, and scalability remain barriers to their widespread adoption.

Although non-PVDF-based ferroelectrics outperform PVDF in traditional metrics, their complex fabrication processes and limited flexibility restrict their use in applications requiring lightweight, adaptable, and biocompatible materials. PVDF:TRFE, while less competitive in polarization and energy density, offers ease of processing, mechanical flexibility, and reliability in wearable and low-power devices. The choice between PVDF and non-PVDF ferroelectrics ultimately depends on application-specific requirements, with PVDF excelling in flexible electronics and bio-inspired technologies, while non-PVDF materials are better suited for high-performance memory applications.

## 6 | Applications of PVDF Beyond Conventional Memory

### 6.1 | Flexible and Ferroelectric Storage

Research on PVDF-based memory devices has focused on enhancing remanent polarization ($P_r$) and current retention. For example, functionalization of PVDF with TrFE has been shown to significantly improve its ferroelectric performance. Inclusion of 20%–30% TrFE reduces the coercive field ($E_c$) to ∼70 MV/m and increases $P_r$ to ∼9 μC/cm$^2$. However, higher TrFE fractions (>50%) destabilize ferroelectric behavior, reducing the hysteresis loop width to resemble relaxor ferroelectrics and ultimately diminishing ferroelectric performance [72–76].

Applications of PVDF-based FeFETs have demonstrated promising results. For instance, Park et al. reported a PVDF-TrFE FeFET device with an organic gate that achieved $P_r$ values of ∼9.8 μC/cm$^2$ and an $I_{on}/I_{off}$ ratio exceeding $10^3$ for 15 h under ambient conditions [27]. The ferroelectric PVDF-TrFE layer contained an improved remanent polarization (9.8 μC/cm$^2$) w.r.t. PVDF-TrFE in FeFETs using conventional gates. With a gate voltage of ±30V and source-drain voltage of −5V, they achieved $I_{on}/I_{off}$ ratio hysteresis larger than 103 for 15h under ambient conditions. Extrapolating the current retention indicates potential stability up to 10 years. However, the operating frequency of the current retention measurements was 1 Hz, meaning that 10 years corresponds to roughly 3.2 $10^8$ completed switching cycles, which is well below the endurance of competing emerging memory devices [28]. Likewise, introducing interfacial layers in FeFETs has been shown to influence the carrier mobility through semiconductor-PVDF interactions, enhancing the process of charge accumulation in the source/drain channel [77]. As a consequence, the reading time of the system has been significantly reduced from 50 to 5 ms. Al-Hazmi et al. investigated doping of $Cu_2O$ nanoparticles into the PVDF-TrFE film, managing to increase the remanent polarization to 11.2 μC/cm$^2$ [56].

Despite these advancements, challenges remain, such as the high electric fields required for polarization inversion, which are inherent to the polymeric unit cell. This higher energy barrier necessitates ultrathin films (0.9–10 μm) to achieve acceptable operating voltages [35, 59].

### 6.2 | Neuromorphic Computing: Emulating Synaptic Plasticity

PVDF has recently gained interest in the field of Neuromorphic (NM) computing, i.e., non-von Neumann memory architectures. In NM computing, the central processing unit and memory are no longer two distinctive components, but instead use a delocalized model, analogous to a simplified brain [17, 78–82]. As a consequence, the high coercive field, slow switching, and low lifetime are less significant. Human reasoning and language abilities rely on pattern recognition of impulses through our neural network. Non-von Neumann systems are neurally inspired architectures, such as neuromorphic and in-memory systems. The neural network embodies one unit, consisting of ∼$10^{11}$ neurons connected by ∼$10^{15}$ synapses, which operate at extremely

low power. Neurons modulate memory through the flow of Calcium ions from pre- to postsynaptic membranes. The interaction strength between two neurons is defined as the synaptic weight and should be able to be modulated in a neuromorphic device. Specifically, the synaptic weight is modulated through a variant time difference between neural spikes, called time-dependent synaptic plasticity (TDSP), which is fundamental for the development of memory systems capable of mimicking brain memory formation, also known as Hebbian learning [83]. Figure 6a,b shows applications of PVDF in neuromorphic computing; diagrams of the devices, SEM images, and ferroelectric responses are included.

In 2018, Tian et al. showed that a FeFET device consisting of a PVDF-TrFE ferroelectric layer and $MoS_2$ channel showed synaptic plasticity behavior, meaning that different conductance states might be regulated through the source and drain terminals. Through polarization reversal, more than one hundred stable conductance states were shown to be accessible, which reflects the artificial synaptic plasticity. The device exhibited stable current retention up to $10^7$ cycles and an operating voltage window of −17 to +12 V. The timescale in which conductance modulation occurred was in the order of ∼100 ms, which is similar to the time lapse with which synaptic events occur in the human brain [80].

In 2019, Majumdar et al. reported an organic tunnel junction for emulating synaptic plasticity, with PVDF as the insulating layer. Through alteration of the voltage amplitude, artificial synapses were implemented with ultrafast response ($10^{-9}$ s) [84]. In 2021, Cheng et al. demonstrated the implementation of synaptic functions of organic ferroelectric tunnel junctions (OFTJs) based on PVDF, which showed long-term potentiation and depression (LTP/LTD), and multi-memory function [85]. In 2023, Jin et al. used a PVDF-TrFE thin film as an interlayer in a $Li^+$ electrolyte-gated transistor. A reduced charge transfer resistance due to ferroelectric polarization of domains was shown, which is crucial to developing an EGT-based artificial synapse [86].

Recently, in 2025, Restuccia et al. tested the synaptic characteristics of PVDF-based organic FETs on training and recognition performance by using 20 x 20 images of handwritten digits. The FETs operated below 7 V, with a dielectric layer thickness of ∼50 nm (Figure 6a) [87]. Later the same year, Poddar et al. developed multifunctional, flexible PCSB composites for use in self-powered piezoelectric sensors and photonic neuromorphic computing by utilizing $CuBO_{2-x}S_x$ and PVDF (PCSB). The optimized piezoelectric nanogenerator produced an electrical output of $V_{OC}$ ∼21.8 V and $I_{SC}$ ∼0.42 μA, under a 4 kHz frequency and 6.1 MPa pressure. Furthermore, the PCSB composite was used to fabricate an optoelectronic synaptic device for neuromorphic computing [88].

These studies collectively highlight a new paradigm that leverages PVDF-based polymers for neuromorphic computing applications, showcasing that despite limitations in conventional memory applications, versatility and potential in enabling artificial synaptic functions, high endurance, ultrafast response times, and multifunctional device integration.

### 6.3 | Sensing Applications: Real-Time Detection and Transient Data Storage

PVDF is a smart material, meaning two or more of its physical properties can be modulated through external stimuli. In addition to ferroelectricity, PVDF demonstrates properties like piezo- and pyroelectricity. Hence, PVDF has been suggested as a pressure (piezoelectric effect) and temperature sensor (pyroelectric response) [89–91]. Smart materials are different from digital memory, but in some way comparable to the CPU: smart sensors receive external stimuli, from which electrical signals can be further processed by an external circuit. The absence of constant operation by voltage pulses is both favorable from an environmental perspective and the desired automatization, i.e., Internet of Things (IoT). The method of communicating data through a smart material (*external stimuli → reading (probing) → processing signal*) is very efficient compared to that of von Neumann computers (*external operation → writing (pulse) → reading (pulse) → processing signal*). Figure 6c,d shows applications of PVDF in sensing applications; diagrams of the devices depicting the sensing mechanism, and the ferroelectric responses are included.

Currently, leading technology companies such as Apple and Samsung are investing in research of novel biomedical devices using smart materials, e.g., smart watches. Such devices can monitor physiological parameters without the physical presence of a doctor, facilitating some degree of self-healthcare. The response of the smart material to an external stimulus is converted to binary data (“0” and “1”) after which it can be communicated to a central unit, such as the smart watch. Some of these monitoring devices require implementation on the skin (or even subdermal), for which PVDF offers the advantages.

In 2016, Yi et al. explored the potential of the piezoelectric property of PVDF for the development of prosthetic limbs. Continuous analogue electric signals were recorded from vibratory stimuli, converted into spike trains using the spiking neural model, and successfully compared to those measured from functional skin of monkeys subjected to the same stimuli [92]. In 2020, Lee et al. reported a flexible, artificial, intrinsic-synaptic tactile sensory organ that mimics synapse-like connections using an organic FET nanocomposite of $BaTiO_3$ nanoparticles into a PVDF-TrFE matrix. The group successfully mimicked the synapse-like connection in a sensory organ, thereby endowing the sensor itself with intrinsic intelligence without linking it to a neuronal processor (Figure 6c) [93].

In 2021, Oh et al., inspired by hippocampal synapses, developed a dual-gate organic synaptic transistor platform with a photoconductive polymer semiconductor, a ferroelectric insulator of PVDF-TrFE, and an extended-gate electrode functionalized with boronic acid, to simultaneously detect the neurotransmitter dopamine and light [94]. In 2025, Liu et al. demonstrated a PVDF-based bionic finger for texture recognition with perception comparable to that of a human finger [95]. Later, the same year, Long et al. synthesized quantum dots functionalized with thiol-terminated PVDF ligands and employed them as the photo-sensitive floating gate in an organic synaptic transistor.

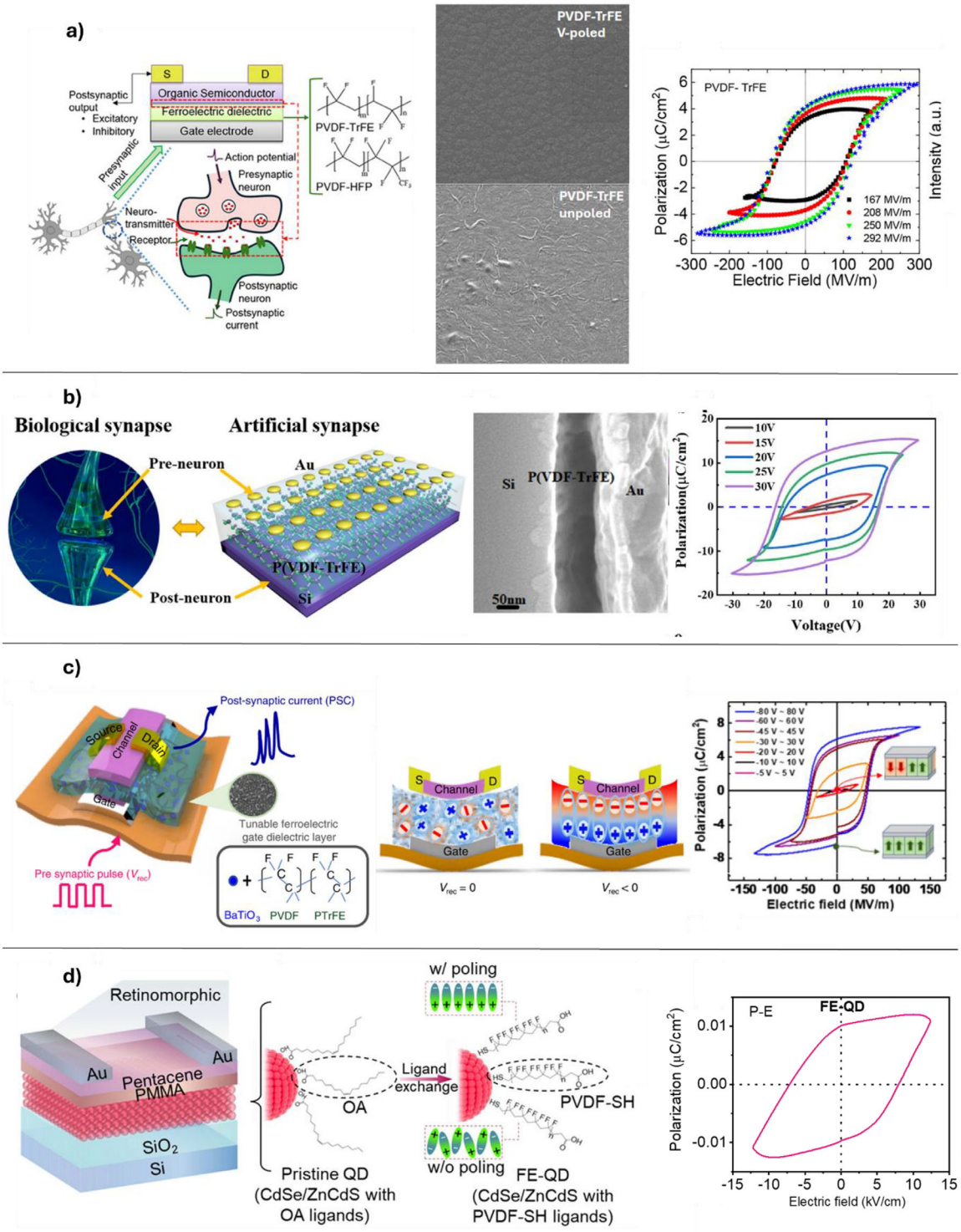


**FIGURE 6** | Applications of PVDF as ferroelectric material in emerging applications: a) Synaptic transistor for neural image recognition networks, adapted with permission. [87] 2025, John Wiley and Sons Ltd. b) Organic memristor based on the P(VDF-TrFE) functional layer for neuromorphic computing, adapted with permission. [83] 2023, KeAi Communications Co. c) Flexible artificial intrinsic-synaptic tactile sensory organ, adapted with permission. [93] 2020, Nature Publishing Group. d) Ferroelectric quantum dots for retinomorphic in-sensor computing, adapted with permission. [96] 2025, Wiley-Blackwell.

According to the authors, when a polarization voltage was applied to the organic synaptic transistors, the generated electric field counteracted exciton confinement and led to 100% accuracy in detecting simulated car motion in low-light conditions (Figure 6d) [96].

These studies highlight the innovative use of PVDF-based materials in bio-inspired technologies, showcasing their ability to emulate complex biological functions such as tactile sensing, neurotransmitter detection, and texture recognition. The advancements in PVDF-based devices demonstrate the potential

to exploit material multi-functionality for smart sensoric systems, such as intelligent prosthetics, adaptive sensory systems, and high-precision motion detection in challenging environments.

## 7 | Summary

The continuous demand for advanced memory technologies has propelled ferroelectric materials into the spotlight due to their potential to address critical challenges such as energy efficiency, scalability, and multifunctionality. This review critically assessed the advancements of polyvinylidene fluoride (PVDF) and its derivatives in the context of emerging memory and related applications.

To address material scientists and chemists, we begin by exploring the fundamental principles of ferroelectricity and memory architectures, highlighting the unique operational mechanisms of ferroelectric memories, such as polarization switching, coercive field, and hysteresis behavior. Conventional ferroelectric materials like lead zirconium titanate (PZT) and hafnium zirconium oxide (HZO) have long dominated memory technologies due to their excellent performance metrics, including high polarization, low coercive fields, and robust cycle endurance. However, other limitations—such as toxicity, brittleness, and high-temperature processing—restrict their use in flexible and biocompatible devices. PVDF, with its mechanical flexibility, lightweight nature, and low-cost processability, has emerged as a promising alternative, particularly for wearable electronics, biomedical devices, and IoT applications where conventional materials fall short.

PVDF's ferroelectric properties arise in the $\beta$-phase, which exhibits the non-centrosymmetric structure required for ferroelectricity. Due to the polymorphic nature of PVDF, achieving reliable high $\beta$-phase content is challenging, as PVDF naturally crystallizes in the non-ferroelectric $\alpha$-phase. Techniques such as mechanical stretching, electrical poling, and copolymerization with trifluoroethylene (TrFE) have been widely adopted to induce and stabilize the $\beta$-phase. However, PVDF's ferroelectric performance is less competitive than that of inorganic ferroelectrics like PZT and HZO for memory applications in terms of polarization strength, energy density, and cycle endurance. Despite these limitations, we argue that versatility in PVDF fabrication routes combined with multifunctional electroactive properties make it an interesting choice for more specialized applications beyond conventional memory technologies.

Studies in the field of neuromorphic computing have shown that PVDF-based materials can mimic biological synaptic functions, enabling artificial synaptic plasticity, ultrafast response times, and long-term potentiation and depression (LTP/LTD). These properties make PVDF an attractive material for non-Von Neumann architectures, which aim to emulate brain-like memory and processing systems. In sensing applications, PVDF's combined piezoelectric and pyroelectric properties have been leveraged for real-time detection and transient data storage. Innovations such as bionic fingers, neurotransmitter detection systems, and intelligent prosthetics showcase PVDF's ability to emulate complex biological functions and its potential for bio-inspired technologies.

The review further examined PVDF-based composites, which integrate organic and inorganic fillers such as $BaTiO_3$, ZnO, and 2D perovskites to enhance PVDF's ferroelectric and piezoelectric properties. These composites have demonstrated significant improvements in polarization, dielectric constant, and energy density, making them promising candidates for advanced memory applications. However, challenges such as filler dispersion, interfacial stability, and scalability remain critical obstacles to their widespread adoption. In contrast, emerging non-PVDF-based ferroelectric materials—such as transition metal dichalcogenides (TMDs), perovskite oxides, and 2D hybrid organic–inorganic perovskites—have shown superior performance in terms of dielectric constants, polarization strength, and thermal stability, making them highly suitable for high-density and energy-efficient memory applications. Nonetheless, their integration into practical devices is constrained by environmental sensitivity and complex fabrication processes.

In conclusion, PVDF and its derivatives represent a versatile and promising class of materials for emerging memory applications, particularly in areas where flexibility, lightweight design, and low-cost processing are critical. While PVDF may not yet match the performance of inorganic ferroelectric materials in traditional metrics, its unique properties enable novel opportunities in flexible electronics, neuromorphic computing, and sensing applications. Future research should focus on addressing challenges related to phase stability, endurance, and scalability, while exploring hybrid materials that combine the strengths of PVDF and inorganic ferroelectrics. With sustained innovation in material engineering and device integration, PVDF-based systems could be poised to play a transformative role in next-generation memory technologies, particularly in applications demanding multifunctionality and adaptability.


### Acknowledgments

Open access funding enabled and organized by Projekt DEAL.


### Conflicts of Interest

The authors declare no conflicts of interest.

### Data Availability Statement

The authors have nothing to report.

### References


1. T. Mikolajick, U. Schroeder, and S. Slesazeck, "The Past, the Present, and the Future of Ferroelectric Memories," *IEEE Transactions on Electron Devices* 67, no. 4 (2020): 1434–1443, https://doi.org/10.1109/TED.2020.2976148.

2. J. S. Meena, S. M. Sze, U. Chand, and T. Tseng, "Overview of Emerging Nonvolatile Memory Technologies," *Nanoscale Research Letters* 9, no. 1 (2014): 526, https://doi.org/10.1186/1556-276X-9-526.

3. S. Hong and N. Setter, "Evidence for Forward Domain Growth Being Rate-Limiting Step in Polarization Switching in <111=-Oriented-$Pb(Zr_{0.45}Ti_{0.55})O_3$ Thin-Film Capacitors," *Applied Physics Letters* 81, no. 18 (2002): 3437–3439, https://doi.org/10.1063/1.1517396.

4. S. J. Kim, J. Mohan, S. R. Summerfelt, and J. Kim, "Ferroelectric $Hf_{0.5}Zr_{0.5}O_2$ Thin Films: A Review of Recent Advances," *JOM* 71, no. 1 (2019): 246–255, https://doi.org/10.1007/s11837-018-3140-5.

5. H. Liu, Y. Ye, X. Zhang, T. Yang, W. Wen, and S. Jiang, "Ferroelectricity in Organic Materials: From Materials Characteristics to De Novo Design," *Journal of Materials Chemistry C* 37, no. 10 (2022): 13676–13689, https://doi.org/10.1039/D2TC01330D.

6. J. A. Rogers, T. Someya, and Y. Huang, "Materials and Mechanics for Stretchable Electronics," *Science* 327, no. 5973 (2010): 1603–1607, https://doi.org/10.1126/science.1182383.

7. M. S. Kim, A. S. Almuslem, W. Babatain, et al., "Beyond Flexible: Unveiling the Next Era of Flexible Electronic Systems," *Advanced Materials* 36, no. 51 (2024): 2406424, https://doi.org/10.1002/adma.202406424.

8. H. Zhu, C. Fu, and M. Mitsuishi, "Organic Ferroelectric Field-Effect Transistor Memories with Poly(Vinylidene Fluoride) Gate Insulators and Conjugated Semiconductor Channels: A Review," *Polymer International* 70, no. 4 (2020): 404–413, https://doi.org/10.1002/pi.6029.

9. S. Horiuchi and Y. Tokura, "Organic Ferroelectrics," *Nature Materials* 7, no. 5 (2008): 357–366, https://doi.org/10.1038/nmat2137.

10. M. Mai, S. Ke, P. Lin, and X. Zeng, "Ferroelectric Polymer Thin Films for Organic Electronics," *Journal of Nanomaterials* 2015 (2015): 1–14, https://doi.org/10.1155/2015/812538.

11. X. Chen, X. Han, and Q. Shen, "PVDF-Based Ferroelectric Polymers in Modern Flexible Electronics," *Advanced Electronic Materials* 3, no. 5 (2017): 1600460, https://doi.org/10.1002/aelm.201600460.

12. Q. Cao, W. Lü, X. R. Wang, et al., "Nonvolatile Multistates Memories for High-Density Data Storage," *ACS Applied Materials and Interfaces* 12, no. 38 (2020): 42449–42471, https://doi.org/10.1021/acsami.0c10184.

13. G. Zhou, Z. Wang, B. Sun, et al., "Volatile and Nonvolatile Memristive Devices for Neuromorphic Computing," *Advanced Electronic Materials* 8, no. 7 (2022): 2101127, https://doi.org/10.1002/aelm.202101127.

14. H. Hidaka, "Applications and Technology Trend in Embedded Flash Memory," in *Embedded Flash Memory for Embedded Systems: Technology, Design for Sub-Systems, and Innovations*, ed. H. Hidaka (Springer, 2018): 7–27, https://doi.org/10.1007/978-3-319-55306-1_2.

15. A. Sheikholeslami and P. G. Gulak, "A survey of Circuit Innovations in Ferroelectric Random-Access Memories," *Proceedings of the IEEE* 88, no. 5 (2000): 667–689, https://doi.org/10.1109/5.849164.

16. R. C. Sousa and I. L. Prejbeanu, "Non-volatile Magnetic Random Access Memories (MRAM)," *Comptes Rendus Physique* 6, no. 9 (2005): 1013–1021, https://doi.org/10.1016/j.crhy.2005.10.007.

17. J. Nau, "Miscellanées Synaptiques, Néo-Zélandaises et Électroniques," *Revue Médicale Suisse* 559 (2017): 878–878, https://doi.org/10.53738/REVMED.2017.13.559.0878.

18. S. Tam, P. Ko, and C. Hu, "Lucky-Electron Model of Channel Hot-Electron Injection in MOSFET'S," *IEEE Transactions on Electron Devices* 31, no. 9 (1984): 1116–1125, https://doi.org/10.1109/T-ED.1984.21674.

19. S. Hong and D. Shin, "NAND Flash-Based Disk Cache Using SLC/MLC Combined Flash Memory", in 2010 International Workshop on Storage Network Architecture and Parallel I/Os (IEEE Computer Society, 2010), 21–30, https://doi.org/10.1109/SNAPI.2010.11.

20. Y. Chiu, "Forever Flash," *IEEE Spectrum* 49, no. 12 (2012): 11–12, https://doi.org/10.1109/MSPEC.2012.6361744.

21. R. Moazzami, "Ferroelectric Thin Film Technology for Semiconductor Memory," *Semiconductor Science and Technology* 10, no. 4 (1995): 375, https://doi.org/10.1088/0268-1242/10/4/001.

22. H. Li, R. Wang, S. Han, and Y. Zhou, "Ferroelectric Polymers for Non-Volatile Memory Devices: A Review," *Polymer International* 69, no. 5 (2020): 533–544, https://doi.org/10.1002/pi.5980.

23. R. Jones, P. Maniar, R. Moazzami, et al., "Ferroelectric Non-Volatile Memories for Low-Voltage, Low-Power Applications," *Thin Solid Films* 270, no. 1 (1995): 584–588, https://doi.org/10.1016/0040-6090(95)06754-X.

24. M. T. Ghoneim and M. M. Hussain, "Review on Physically Flexible Nonvolatile Memory for Internet of Everything Electronics," *Electronics* 4, no. 3 (2015): 3, https://doi.org/10.3390/electronics4030424.

25. T. Tsakalakos, "Nanostructures and Nanotechnology: Perspectives and New Trends," in *Nanostructures: Synthesis, Functional Properties and Applications*, ed. T. Tsakalakos, I. A. Ovid'ko, and A. K. Vasudevan. (Springer, 2003): 1–36, https://doi.org/10.1007/978-94-007-1019-1_1.

26. A. Bussmann-Holder and N. Dalal, "Order/Disorder Versus or with Displacive Dynamics in Ferroelectric Systems," in *Ferro- and Antiferroelectricity: Order/Disorder Versus Displacive*, ed. N. S. Dalal, A. Bussmann-Holder. (Springer, 2007): 1–21, https://doi.org/10.1007/430_2006_045.

27. Y. J. Park, H. J. Jeong, J. Chang, S. J. Kang, and C. Park, "Recent Development in Polymer Ferroelectric Field Effect Transistor Memory," *Journal of Semiconductor Technology and Science* 8, no. 1 (2008): 51–65, https://doi.org/10.5573/JSTS.2008.8.1.051.

28. S. J. Kang, I. Bae, Y. J. Park, et al., "Non-Volatile Ferroelectric Poly(Vinylidene Fluoride-Co-Trifluoroethylene) Memory Based on a Single-Crystalline Tri-Isopropylsilylethynyl Pentacene Field-Effect Transistor," *Advanced Functional Materials* 19, no. 10 (2009): 1609–1616, https://doi.org/10.1002/adfm.200801097.

29. F. Bauer, "Relaxor Fluorinated Polymers: Novel Applications and Recent Developments," *IEEE Transactions on Dielectrics and Electrical Insulation* 17, no. 4 (2010): 1106–1112, https://doi.org/10.1109/TDEI.2010.5539681.

30. B. B. Tian, J. L. Wang, S. Fusil, et al., "Tunnel Electroresistance Through Organic Ferroelectrics," *Nature Communications* 7, no. 1 (2016): 11502, https://doi.org/10.1038/ncomms11502.

31. A. Ruff, A. Loidl, and S. Krohns, "Multiferroic Hysteresis Loop," *Materials* 10, no. 11 (2017): 11, https://doi.org/10.3390/ma10111318.

32. R. Tadros-Morgane, T. Steinmetz, R. Florange, and H. Kliem, "Polarization Switching in Langmuir-Blodgett PVDF Copolymer Thin Films," *Ferroelectrics* 304, no. 1 (2004): 47–49, https://doi.org/10.1080/00150190490454486.

33. E. Schreck and K. Dransfeld, "Fast polarization Reversal in Thin Copolymer Films of Vinylidene Fluoride-Trifluoroethylene," *Applied Physics A* 53, no. 5 (1991): 457–461, https://doi.org/10.1007/BF00348162.

34. R. C. G. Naber, K. Asadi, P. W. M. Blom, D. M. de Leeuw, and B. de Boer, "Organic Nonvolatile Memory Devices Based on Ferroelectricity," *Advanced Materials* 22, no. 9 (2010): 933–945, https://doi.org/10.1002/adma.200900759.

35. G. Vizdrik, S. Ducharme, V. M. Fridkin, and S. G. Yudin, "Kinetics of Ferroelectric Switching in Ultrathin Films," *Physical Review B* 68, no. 9 (2003): 094113, https://doi.org/10.1103/PhysRevB.68.094113.

36. H. Kohlstedt, Y. Mustafa, A. Gerber, et al., "Current Status and Challenges of Ferroelectric Memory Devices," *Microelectronic Engineering* 80 (2005): 296–304, https://doi.org/10.1016/j.mee.2005.04.084.

37. K. Zeissler, "Better FeRAM With Antiferroelectric Capacitors," *Nature Electronics* 4, no. 12 (2021): 860–860, https://doi.org/10.1038/s41928-021-00700-y.

38. K. Uchino, "Future of Ferroelectric Devices," in *Ferroelectric Devices*, 2nd ed. (CRC Press, 2009).

39. Q. Pan, Z. Gu, R. Zhou, et al., "The past 10 Years of Molecular Ferroelectrics: Structures, Design, and Properties," *Chemical Society Reviews* 53 (2024): 5781–5861, https://doi.org/10.1039/D3CS00262D.

40. S. Deornellas, P. Rajora, and A. Cofer, "Challenges for Plasma Etch Integration of Ferroelectric Capacitors in FeRAM's and DRAM's," *Integrated Ferroelectrics* 17, no. 1–4 (1997): 395–402, https://doi.org/10.1080/10584589708013014.

41. D. Wang, S. Yang, J. Liu, D. Wang, and Z. Mi, "Perspectives on Nitride Ferroelectric Semiconductors: Challenges and Opportunities," *Applied Physics Letters* 124, no. 15 (2024): 150501, https://doi.org/10.1063/5.0206005.

42. M. Guo, J. Jiang, J. Qian, et al., "Flexible Robust and High-Density FeRAM From Array of Organic Ferroelectric Nano-Lamellae by Self-

Assembly," *Advanced Science* 6, no. 6 (2019): 1801931, https://doi.org/10.1002/advs.201801931.

43. A. J. Lovinger, "Ferroelectric Polymers," *Science* 220, no. 4602 (1983): 1115–1121, https://doi.org/10.1126/science.220.4602.1115.

44. X. Wang, S. Zhang, Y. Hu, W. Zhou, and X. Huang, "Piezoelectric Polymers and their Applications in Antimicrobial Fields," *Materials Chemistry Frontiers* 9, no. 5 (2025): 754–771, https://doi.org/10.1039/D4QM00930D.

45. A. Frick, W. A. van Vliet, A. Žukauskaitė, et al., "Volumetric 3D-Printed Piezoelectric Polymer Films," *Advanced Materials Technologies* 9, no. 6 (2024): 2301469, https://doi.org/10.1002/admt.202301469.

46. P. N. Bernal, S. Florczak, S. Inacker, et al., "The Road Ahead in Materials and Technologies for Volumetric 3D Printing," *Nature Reviews Materials* (2025): 1–16, https://doi.org/10.1038/s41578-025-00785-3.

47. H. Sun, J. Zhu, D. Baumann, et al., "Hierarchical 3D Electrodes for Electrochemical Energy Storage," *Nature Reviews Materials* 4, no. 1 (2019): 45–60, https://doi.org/10.1038/s41578-018-0069-9.

48. L. Ruan, X. Yao, Y. Chang, L. Zhou, G. Qin, and X. Zhang, "Properties and Applications of the $\beta$ Phase Poly(Vinylidene Fluoride)," *Polymers* 10, no. 3 (2018): 1–27, https://doi.org/10.3390/polym10030228.

49. R. P. Vijayakumar, D. V. Khakhar, and A. Misra, "Studies on a to b Phase Transformations in Mechanically Deformed PVDF Films," *Journal of Applied Polymer Science* 117 (2010): 3491–3497, https://doi.org/10.1002/app.32218.

50. D. Han and B. Park, "Nonvolatile Ferroelectric Memory Transistors Using PVDF, P(VDF-TrFE) and Blended PVDF/P(VDF-TrFE) Thin Films," in *Ferroelectric-Gate Field Effect Transistor Memories: Device Physics and Applications in Topics in Applied Physics –in Topics in Applied Physics*, ed. B. E. Park, H. Ishiwara, M. Okuyama, S. Sakai, and S. M. Yoon, (Springer, 2020), 177–194, https://doi.org/10.1007/978-981-15-1212-4_9.

51. L. Maiolo, F. Maita, A. Pecora, et al., "Flexible PVDF-TrFE Pyroelectric Sensor Integrated on a Fully Printed P-channel Organic Transistor," *Procedia Engineering* 47 (2012): 526–529, https://doi.org/10.1016/j.proeng.2012.09.200.

52. S. Abdalla, A. Obaid, and F. M. M. Al-Marzouki, "Preparation and Characterization of Poly(Vinylidene Fluoride): A High Dielectric Performance Nano-Composite For Electrical Storage," *Results in Physics* 6 (2016): 617–626, https://doi.org/10.1016/j.rinp.2016.09.003.

53. N. Ramer and K. Stiso, "Comparison of Polarization and Born Effective Charges in Alternatively-Deflected Zigzag and Planar-Zigzag $\beta$-Poly(Vinylidene Fluoride)," *Condensed Matter* (2004), https://doi.org/10.48550/arXiv.cond-mat/0411564.

54. S. M. Nakhmanson, M. B. Nardelli, and J. Bernholc, "Collective Polarization Effects in $\beta$-Polyvinylidene Fluoride and its Copolymers with Tri- and Tetrafluoroethylene," *Physical Review B* 72, no. 11 (2005): 115210, https://doi.org/10.1103/PhysRevB.72.115210.

55. S. Chen, K. Yao, F. E. H. Tay, and L. L. S. Chew, "Comparative Investigation of the Structure and Properties of Ferroelectric Poly(Vinylidene Fluoride) and Poly(Vinylidene Fluoride–Trifluoroethylene) Thin Films Crystallized On Substrates," *Journal of Applied Polymer Science* 116, no. 6 (2010): 3331–3337, https://doi.org/10.1002/app.31794.

56. F. S. Al-Hazmi, D. M. de Leeuw, A. A. Al-Ghamdi, and F. S. Shokr, "Synthesis and Characterization of novel $Cu_2O$/PVDF Nanocomposites for Flexible Ferroelectric Organic Electronic Memory Devices," *Current Applied Physics* 17, no. 9 (2017): 1181–1188, https://doi.org/10.1016/j.cap.2017.05.011.

57. P. D. Richardson, "Piezoelectric Polymers," *IEEE Engineering in Medicine and Biology Magazine* 8, no. 2 (1989): 14–16, https://doi.org/10.1109/51.31634.

58. A. Gerber, M. Fitsilis, R. Waser, et al., "Ferroelectric Field Effect Transistors Using Very Thin Ferroelectric Polyvinylidene Fluoride Copolymer Films as Gate Dielectrics," *Journal of Applied Physics* 107 (2010): 124119, https://doi.org/10.1063/1.3437638.

59. T. Nakajima, R. Abe, Y. Takahashi, and T. Furukawa, "Intrinsic Switching Characteristics of Ferroelectric Ultrathin Vinylidene Fluoride/Trifluoroethylene Copolymer Films Revealed Using Au Electrode," *Japanese Journal of Applied Physics* 44 (2005): L1385, https://doi.org/10.1143/JJAP.44.L1385.

60. X. Zhang, W. Xia, J. Xing, Y. Feng, and D. Lu, "Research Progress of Polyvinylidene Fluoride and its Copolymer Piezoelectric Composites," *Acta Materiae Compositae Sinica* 38, no. 4 (2021): 997–1019, https://doi.org/10.13801/j.cnki.fhclxb.20201210.004.

61. R. Gregorio, M. Cestari, and F. Bernardino, "Dielectric Behavior of Thin Films of $\beta$-PVDF/PZT and $\beta$-PVDF/$BaTiO_3$ Composites," *Journal of Materials Science* 31 (1996): 2925–2930, https://doi.org/10.1007/BF00356003.

62. Y. Park, Y. Shin, J. Park, et al., "Ferroelectric Multilayer Nanocomposites with Polarization and Stress Concentration Structures for Enhanced Triboelectric Performances," *ACS Nano* 14, no. 6 (2020): 7101–7110, https://doi.org/10.1021/acsnano.0c01865.

63. B. Joshi, J. Seol, E. Samuel, et al., "Supersonically sprayed PVDF and ZnO flowers with built-in nanocuboids for wearable piezoelectric nanogenerators," *Nano Energy* 112 (2023): 108447, https://doi.org/10.1016/j.nanoen.2023.108447.

64. A. Sahoo, T. Paul, N. H. Makani, S. Maiti, and R. Banerjee, "High Piezoresponse in Low-Dimensional Inorganic Halide Perovskite for Mechanical Energy Harvesting," *Sustainable Energy Fuels* 6 (2022): 4484–4497, https://doi.org/10.1039/D2SE00786J.

65. Z. Chen, M. Zhang, Y. Hu, S. Wang, H. Gu, and J. Xiong, "Ultrahigh Energy Harvesting Ability of PVDF Incorporated with 2D Halide Perovskite Nanosheets via Interface Effect," *Chemical Engineering Journal* 497, no. 1 (2024): 154558.

66. J. Son, M. Lee, A. Sannyal, et al., "Self-Rectifying Resistive Memory with a Ferroelectric and 2D Perovskite Lateral Heterostructure," *ACS Nano* 19, no. 11 (2025): 10796–10806, https://doi.org/10.1021/acsnano.4c07869.

67. B. Chen, W. Zhu, T. Wang, et al., "Ultrahigh Energy Storage Capacitors Based on Freestanding Single-Crystalline Antiferroelectric Membrane/PVDF Composites," *Advanced Functional Materials* 33, no. 36 (2023): 2302683, https://doi.org/10.1002/adfm.202302683.

68. Q. H. Wang, K. Kalantar-Zadeh, A. Kis, J. N. Coleman, and M. S. Strano, "Electronics and Optoelectronics of Two-Dimensional Transition Metal Dichalcogenides," *Nature Nanotechnology* 7 (2012): 699, https://doi.org/10.1038/nnano.2012.193.

69. S. R. Bakaul, C. R. Serrao, O. Lee, et al., "High Speed Epitaxial Perovskite Memory on Flexible Substrates," *Advanced Materials* 29, no. 11 (2017): 1605699, https://doi.org/10.1002/adma.201605699.

70. M. Zhang, Y. Wei, C. Liu, et al., "Perspectives on MXene-PZT Based Ferroelectric Memristor in Computation in Memory Applications," *Applied Physics Letters* 123 (2023): 060501, https://doi.org/10.1063/5.0159338.

71. H. Ni, Q. Zhou, J. Luo, et al., "Lone Pair Expression in Fluorinated Two-Dimensional Hybrid Perovskite Enables Multiaxial Ferroelectricity and Nonlinear Optical Response," *Nature Communications* 16 (2025): 7760, https://doi.org/10.1038/s41467-025-63134-6.

72. E. Bellet-Amalric and J. F. Legrand, "Crystalline Structures and Phase Transition of the Ferroelectric P(VDF-TrFE) Copolymers, a Neutron Diffraction Study," *European Physical Journal B* 3, no. 2 (1998): 225–236, https://doi.org/10.1007/s100510050307.

73. B. Ploss and B. Ploss, "Dielectric Nonlinearity of PVDF–TrFE Copolymer," *Polymer* 41, no. 16 (2000): 6087–6093, https://doi.org/10.1016/S0032-3861(99)00861-7.

74. W. J. Hu, D. Juo, L. You, et al., "Universal Ferroelectric Switching Dynamics of Vinylidene Fluoride-Trifluoroethylene Copolymer Films," *Scientific Reports* 4, no. 1 (2014): 4772, https://doi.org/10.1038/srep04772.

75. T. Furukawa and Y. Takahashi, "Ferroelectric and Antiferroelectric Transitions in Random Copolymers of Vinylidene Fluoride and Trifluoroethylene," *Ferroelectrics* 264, no. 1 (2001): 81–90, https://doi.org/10.1080/00150190108008551.

76. Y. Liu, Z. Han, W. Xu, A. Haibibu, and Q. Wang, "Composition-Dependent Dielectric Properties of Poly(Vinylidene Fluoride-Trifluoroethylene)s Near the Morphotropic Phase Boundary," *Macromolecules* 17, (2024): 6741–6747, https://doi.org/10.1021/acs.macromol.9b01403.

77. H. Sun, Q. Wang, Y. Li, et al., "Boost Up Carrier Mobility for Ferroelectric Organic Transistor Memory via Buffering Interfacial Polarization Fluctuation," *Scientific Reports* 4, no. 1 (2014): 7227, https://doi.org/10.1038/srep07227.

78. Y. Park, M. Kim, and J. Lee, "Emerging Memory Devices for Artificial Synapses," *Journal of Materials Chemistry C* 8, no. 27 (2020): 9163–9183, https://doi.org/10.1039/D0TC01500.

79. J. Hasler and B. Marr, "Finding a Roadmap to Achieve Large Neuromorphic Hardware Systems," *Frontiers in Neuroscience* 7 (2013): 118, https://doi.org/10.3389/fnins.2013.00118.

80. B. Tian, L. Liu, M. Yan, et al., "A Robust Artificial Synapse Based on Organic Ferroelectric Polymer," *Advanced Electronic Materials* 5, no. 1 (2019): 1800600, https://doi.org/10.1002/aelm.201800600.

81. C. D. Schuman, T. E. Potok, R. M. Patton, et al., "A Survey of Neuromorphic Computing and Neural Networks in Hardware," arXiv (2017): arXiv:1705.06963, https://doi.org/10.48550/arXiv.1705.06963.

82. D. Wang, S. Hao, B. Dkhil, B. Tian, and C. Duan, "Ferroelectric Materials for Neuroinspired Computing Applications," *Fundamental Research* 4, no. 5 (2024): 1272–1291, https://doi.org/10.1016/j.fmre.2023.04.013.

83. Q. Li, Y. Liu, Y. Cao, et al., "Ferroelectric Artificial Synapse for Neuromorphic Computing and Flexible Applications," *Fundamental Research* 3, no. 6 (2023): 960–966, https://doi.org/10.1016/j.fmre.2022.02.004.

84. X. Niu, B. Tian, Q. Zhu, B. Dkhil, and C. Duan, "Ferroelectric Polymers for Neuromorphic Computing," *Applied Physics Reviews* 9, no. 2 (2022): 021309, https://doi.org/10.1063/5.0073085.

85. L. Cheng, H. Sun, J. Xu, et al., "Emulation of Synaptic Behavior by Organic Ferroelectric Tunnel Junctions," *Physics Letters A* 392 (2021): 127138, https://doi.org/10.1016/j.physleta.2021.127138.

86. M. Jin, H. Lee, J. H. Lee, et al., "Ferroelectrically Modulated Ion Dynamics in $Li^+$ Electrolyte-Gated Transistors for Neuromorphic Computing," *Applied Physics Reviews* 10 (2023): 011407, https://doi.org/10.1063/5.0130742.

87. E. Restuccia, A. Ghobadi, and S. Guha, "Organic Ferroelectric Synaptic Transistors for Neural Image Recognition Networks," *Advanced Materials Interfaces* 12, no. 13 (2025): 2401035, https://doi.org/10.1002/admi.202401035.

88. S. Poddar, P. Das, S. Bhattacharjee, and K. K. Chattopadhyay, "Inversion Symmetry-Broken $CuBO_2$ Delafossite Through Anionic Site Doping for Improved Piezoelectric Composites with PVDF and its Application in Nanogenerators and Optoelectronic Neuromorphic Computing," *Journal of Materials Chemistry A* 13 (2025): 28451–28470, https://doi.org/10.1039/D5TA02437D.

89. G. Wang, T. Liu, X. Sun, et al., "Flexible Pressure Sensor Based on PVDF Nanofiber," *Sensors and Actuators A: Physical* 280 (2018): 319–325, https://doi.org/10.1016/j.sna.2018.07.057.

90. W. Li, E. Iranmanesh, J. A. Weldon, and K. Wang, "Single-Pixel Tactile Sensor Based on Piezoelectric-Charge-Gated Thin-Film Transistor," in 2016 IEEE International Conference on Advanced Intelligent Mechatronics (AIM), (IEEE, 2016), 805–809, https://doi.org/10.1109/AIM.2016.7576867.

91. S. A. Pullano, I. Mahbub, S. K. Islam, and A. S. Fiorillo, "PVDF Sensor Stimulated by Infrared Radiation for Temperature Monitoring in Microfluidic Devices," *Sensors* 17, no. 4 (2017): 4, https://doi.org/10.3390/s17040850.

92. Z. Yi and Y. Zhang, "Bio-Inspired Tactile FA-I Spiking Generation Under Sinusoidal Stimuli," *Journal of Bionic Engineering* 13 (2016): 612–621, https://doi.org/10.1016/S1672-6529(16)60332-3.

93. Y. R. Lee, T. Q. Trung, B. Hwang, and N. Lee, "A Flexible Artificial Intrinsic-Synaptic Tactile Sensory Organ," *Nature Communications* 11 (2020): 2753, https://doi.org/10.1038/s41467-020-16606-w.

94. H. R. Lee, D. Lee, and J. Oh, "A Hippocampus-Inspired Dual-Gated Organic Artificial Synapse for Simultaneous Sensing of a Neurotransmitter and Light," *Advanced Materials* 33, no. 17 (2021): 2100119, https://doi.org/10.1002/adma.202100119.

95. Z. Liu, X. Wang, G. Xiang, Z. Wang, Y. Shao, and H. Liu, "A Neuromorphic Tactile Perception System Based on Spiking Neural Network for Texture Recognition," paper presented at Intelligent Robotics and Applications: 17th International Conference, ICIRA 2024, Proceedings, Part IX, 176–191, July 31–August 2, 2024.

96. T. Long, H. Zhou, J. Ko, et al., "Ferroelectric Quantum Dots for Retinomorphic In-Sensor Computing", *Advanced Materials* (2025): 04117, https://doi.org/10.1002/adma.202504117.

97. eds. T. Tsakalakos, I. A. Ovid'ko, and A. K. Vasudevan, *Nanostructures: Synthesis, Functional Properties and Applications* (Springer, 2003), https://doi.org/10.1007/978-94-007-1019-1.

98. G. Sun, "Exploring Memory Hierarchy Design with Emerging Memory Technologies," in *Lecture Notes in Electrical Engineering* (Springer International Publishing, 2014), https://doi.org/10.1007/978-3-319-00681-9.

99. M. Imani, S. Patil, and T. Rosing, "Low power Data-Aware STT-RAM Based Hybrid Cache Architecture," in 2016 17th International Symposium on Quality Electronic Design (ISQED) (IEEE, 2016), 88–94.

100. A. C. Hinckley, C. Wang, R. Pfattner, et al., "Investigation of a Solution-Processable, Nonspecific Surface Modifier for Low Cost, High Work Function Electrodes," *ACS Applied Materials and Interfaces* 8, no. 30 (2016): 19658–19664, https://doi.org/10.1021/acsami.6b05348.

101. I. Katsouras, K. Asadi, M. Li, et al., "The Negative Piezoelectric Effect of the Ferroelectric Polymer Poly(Vinylidene Fluoride)," *Nature Materials* 15, no. 1 (2016): 78–84, https://doi.org/10.1038/nmat4423.